An adaptive finite element method for computing emergency manoeuvres of ground vehicles in complex driving scenarios

Kanarachos, S and Alirezaei , M.

Title:

An adaptive finite element method for computing emergency maneuvers of ground vehicles with arbitrary boundary conditions

Abstract

In emergency maneuvers a vehicle has to avoid one or more obstacles, stay within road boundaries, satisfy acceleration and jerk limits, fulfill stability requirements and respect vehicle system dynamics limitations. Solving such a problem in real-time is difficult and as a result various approaches, which usually relax the problem, have been proposed until now. In this study, a new method for computing emergency paths with arbitrary boundary conditions is presented. The method recasts the dynamic optimization problem into a constrained nonlinear algebraic one using a finite element concept. An empirical formula which adapts the length of the finite elements is used to optimize the vehicle's performance. The proposed approach is evaluated in Matlab & Carsim simulation environments for different driving scenarios. The results show that with the proposed approach complex emergency maneuvers are effectively planned with improved performance compared to other known methods.

Keywords: emergency path planning, finite elements, dynamic optimization, model based constraints

1. Introduction

Corresponding author: Stratis Kanarachos,

The main cause of car crashes is human errors in judgment and decision making. Commercially available collision mitigation systems such as the Autonomous Emergency Braking (AEB) will undoubtedly improve current road safety standards by reducing the

number of deaths and severe injuries. Next generation ADAS will bring us even closer to the zero fatalities target since they will have autonomous collision avoidance capability by planning and controlling the lateral motion of a vehicle in space and time. This paper focuses on the Emergency Path (EP) planning part for which various approaches have been proposed until now: polynomials, elastic bands, splines, sigmoid functions, maneuver automatons and model predictive control (Brandt et al, 2007).

An EP besides avoiding obstacles and remaining within the road boundaries needs to fulfill constraints which are linked to the vehicle's capabilities. Snider (2009) has studied and assessed the performance of a number of path tracking controllers including kinematic, linear quadratic regulator (LQR), optimal preview and nonlinear model predictive control. One of the study's main outcomes was that irrespectively of the controller if the path is too abrupt with respect to vehicle dynamics then it can't be successfully tracked . In the same line, Gray et al (2012) has concluded that the trajectory generated by a point-mass path planner although real-time capable was not always feasible. The lower level tracking controller could not follow the planned path and obstacle collisions were observed in conditions where the obstacle could have been avoided. Thus, they proposed a path planner based on motion primitives which respect a priori the vehicle dynamics constraints. The main drawback is that motion primitives aren't easily applicable in case EP has arbitrary geometry.

A method proposed by Shim et al [2010] generates smooth paths by parameterization of the EP using two sixth order polynomials. The polynomials' unknown coefficients are computed a) by determining the position, velocity and acceleration at the beginning and end of the trajectory and b) by solving a minimization problem which seeks to minimize

the travel distance. The performance of the path planner was evaluated in a simulation environment considering a model predictive path tracking controller. One of the disadvantages of higher order polynomials is that they can show oscillatory behavior. In order to tackle the problem Keller et al. (2011) suggested a sigmoidal - polynomial approach. EP was parameterized by a polynomial of 7^{th} degree which coefficients are determined based on several constraints regarding maximum lateral acceleration, derivatives of the lateral offset and curvature. Maneuvering time was approximated based on a shape factor which is distinctive for 7^{th} order polynomials and straight line emergency maneuvers. System performance has been evaluated both computationally and experimentally.

Isermann et al. (2012) observed that emergency maneuvers form an "S" shape and employed a sigmoid function to parameterize the EP. The sigmoidal is described by three parameters which are calculated by solving a system of nonlinear algebraic equations. The solution results in an evasive path with minimal length which respects different system limits such as maximum lateral acceleration, maximal jerk and dynamics of the steering actuator. The method has been evaluated both experimentally and computationally. Disadvantage of the method is that it has been developed for straight paths only.

The necessity to plan in real time EPs for complex driving scenarios with arbitrary conditions was our main motivation. In the present work a methodological framework is provided for this purpose. Inspired by collocation schemes developed in other engineering fields (Yang et al., 2014, Solsvik and Jacobsen, 2012, Vaferi et al., 2012, Arora et al., 2006), we recast the original dynamic optimization problem into a nonlinear

algebraic one by decomposing the EP into a predefined number of standardized finite elements. In the first iteration a rough solution of the problem is obtained by solving a linear system of equations. The solution includes the trajectory, its dynamic properties and the required inputs. System's constraints, such as tire forces saturation or actuators limits, are formulated using a model based approach and expressed through the elements' nodal unknowns. The feasibility of the resulting EP is easily checked with a limited number of algebraic calculations. In the second step the dynamic properties of the EP are optimized using an empirical formula while in the third step the minimum maneuvering time is sought using a novel optimization approach. To our knowledge this method is proposed for the first time.

The rest of the paper is organized as follows. In Sections 2 and 3 the vehicle model used and the finite element concept which recasts the dynamic optimization problem into a nonlinear algebraic one are discussed respectively. In section 4 the adaptive solution methodology is presented. In Section 5 the EP planner is evaluated and compared with an alternative method known from the literature for different driving scenarios. In section 6 the robustness of the proposed method is evaluated in case the friction coefficient estimation is uncertain. The analysis and evaluation is performed in Matlab & Carsim simulation environments. In Section 7 conclusions and future research directions are drawn.

2. Mathematical model

Vehicle model and model based constraints

Since a very detailed vehicle model can be difficult to obtain and use, the method described in this paper makes use of a model that approximates vehicle motion. Furthermore, it is assumed that the vehicle is equipped with an Electronic Stability Control (ESC) system, such as the one described in Rajamani, 2012. Furthermore, we assume that the ESC system utilizes the same limit $r_{\max 0}$ as the path tracking system. This effectively means that any commanded yaw rate $r_{des} > r_{\max 0}$ will cause ESC's system activation and thus bring the vehicle from a path tracking to a stability mode.

The two track vehicle model (TTVM), shown in Figure 1, is employed to derive the equations of motion described by forward velocity u_f, lateral velocity v and yaw rate r (Pacejka, 2005).

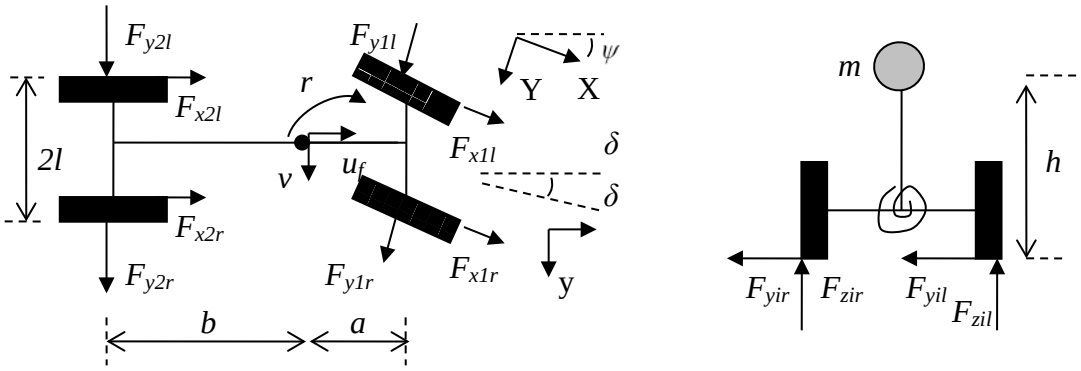

Figure 1. Top view (left) and front view (right) of TTVM

For simplification reasons shock absorbers and suspension springs are neglected. Also neglected are roll angle, steer angle and roll axis inclination which are assumed small enough. Effects of additional steer angles due to suspension kinematics and steer compliance are ignored (Pacejka, 2005). The equations of motion, Eq. (1)-(3), are:

$$m \cdot \left(\dot{u}_f - r \cdot v \right) = \sum F_x = F_{x1} - F_{y1} \cdot \delta + F_{x2} \qquad (1)$$

$$m \cdot \left(\dot{v} + r \cdot u_f \right) = \sum F_y = F_{x1} \cdot \delta + F_{y1} + F_{y2} \tag{2}$$

$$I_z \cdot \dot{r} = \sum M = a \cdot F_{y1} - b \cdot F_{y2} \tag{3}$$

Vehicle velocities $\dot{X}$ and $\dot{Y}$ in the global coordinate system O(X,Y) are a function of local velocities u_f and v (expressed in the vehicle coordinate system o(x,y) and angle ψ (shown in Figure 1). The transformation from one coordinate system to the other is obtained by:

$$\begin{bmatrix} \dot{X} \\ \dot{Y} \\ \dot{\psi} \end{bmatrix} = \begin{bmatrix} \cos\psi & -\sin\psi & 0 \\ \sin\psi & \cos\psi & 0 \\ 0 & 0 & 1 \end{bmatrix} \cdot \begin{bmatrix} u_f \\ v \\ r \end{bmatrix} \tag{4}$$

The vehicle's trajectory (X, Y), expressed in the global coordinate system, is:

$$X = \int_0^T \dot{X} \cdot \cos\psi \cdot dt \tag{5}$$

$$Y = \int_0^T \dot{Y} \cdot \sin\psi \cdot dt \tag{6}$$

where T is the maneuvering time.

Vehicle's yaw rate r is limited either because of the available tire-road friction or because of stability reasons. In the first case, the yaw rate limit $r_{\max 0}$ results from Equation (2):

$$a_y = \dot{v} + u_f \cdot r \approx u_f \cdot r \le a_{y\max} = \mu \cdot m \cdot g \Rightarrow \tag{7}$$

$$r_{\max 0} = \frac{c_0 \cdot \mu \cdot m \cdot g}{u_f} \tag{8}$$

where g is the gravitational acceleration and $c_0 \in [0.85, 0.95]$ a coefficient compensating the influence of vehicle slip angle β which is omitted in calculations (Rajamani, 2012).

In the second case, for stability reasons, the load transfer δF_{zi} occurring during cornering is limited so that a minimum wheel normal load exists. By applying moment equilibrium in the roll direction we get:

$$\delta F_{zi} = \frac{m \cdot a_y \cdot h}{2 \cdot l} \leq \delta F_{zi\_\max} \tag{9}$$

where h is the height of center of gravity. Combining Equations (7) and (9) gives the yaw rate's $r_{\max 1}$ upper bound:

$$r_{\max 1} = \frac{2 \cdot c_1 \cdot \delta F_{zi\_\max} \cdot l}{u_f \cdot m \cdot h} \tag{10}$$

Coefficient $c_1 \in [0.85, 0.95]$ accounts for the influence of neglected vehicle slip angle (Rajamani, 2012). The term $\delta F_{zi\_\max}$ accounts for the neglected roll motion and depends on the specific vehicle suspension and road's bank angle. It can be derived experimentally or by detailed vehicle dynamics simulations using e.g. a fishhook maneuver (Shim, 2007). In Table 1 the vehicle parameters used in the study are listed.

Table 1 Vehicle parameters.

Name	**Parameter**	**Value**
Vehicle mass	m [kg]	1737
Distance from ground to CG	h [m]	0.58
Moment of inertia - to z axis	I_z [kgm^2]	2877
Half length of the wheel axle	l [m]	0.765
Distance of front axle from cog	a [m]	1.3

Tire model & yaw rate limit

Tire forces are mathematically described using the well-known Magic Formula model. For pure side slip a_s the tire's lateral force F_{y0} is:

$$F_{y0}(\alpha_S) = D \cdot \sin\left(C \cdot \arctan\left(B \cdot \alpha_S - E \cdot \left(B \cdot \alpha_S - \arctan\left(B \cdot \alpha_S\right)\right)\right)\right) \tag{11}$$

where $\alpha_S = \tan(\alpha)$ is the slip angle, $D = \mu \cdot F_z$ the peak value, C the shape factor, $B = \frac{C_{F\alpha}}{C \cdot D}$ the stiffness factor and E the curvature factor. A graphical illustration of lateral force F_y versus slip angle α for four different normal loads is shown in Figure 2. We denote with $\alpha_{\max}(\mu, F_z)$ the tire slip angle for which the lateral force is maximized $F_{y_{\max}}$. In Table 2 the tire parameters used in the study are listed.

Table 2 Tire parameters.

Name	**Parameter**	**Value**
Shape factor	C	1.3
Tire-road friction coefficient	M	0.5
Curvature factor	E	-3
Stifness coefficient	$C_{F\alpha} = c_1 \cdot \sin\left(2 \cdot \arctan\left(\frac{F_z}{c_2}\right)\right)$	
Maximum cornering stiffness [N/rad]	c_1	60000
Load at max. cornering stiffness [N]	c_2	4000

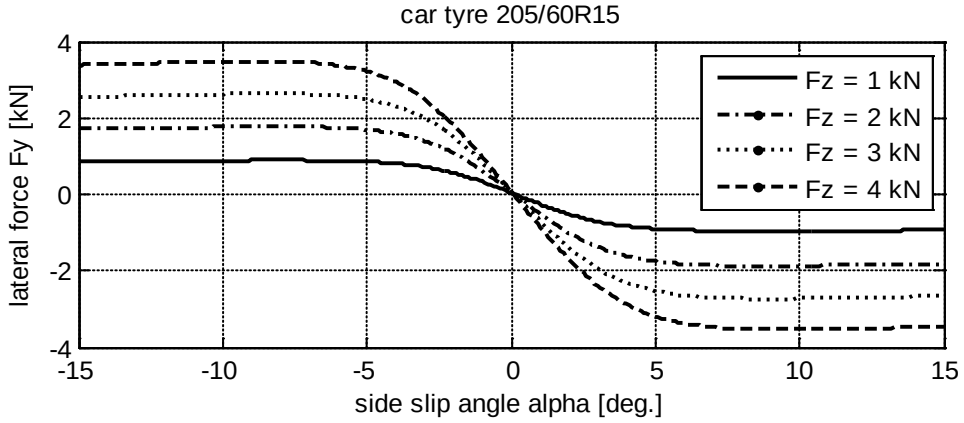

Figure 2. Lateral force versus tire slip angle for different normal loads

Tire slip angles α_1 and α_2 on front and rear wheels are considered small ($\sin \alpha_i \approx \alpha_i$) and expressed as:

$$\alpha_1 = \delta - \frac{1}{u_f} \cdot (v + a \cdot r) \tag{12}$$

$$\alpha_2 = -\frac{1}{u_f} \cdot (v - b \cdot r) \tag{13}$$

where δ is the steer angle. We assume equal slip angles at both left and right wheels ($\alpha_{1r} = \alpha_{1l} = \alpha_1$ and $\alpha_{2r} = \alpha_{2l} = \alpha_2$) which is a valid assumption when $l \cdot |r| << u_f$ (Pacejka, 2005). From Equation (12) and (13) and assuming for simplification reasons that velocity *v* is negligible we get respectively:

$$\delta_{\max} = \alpha_{\max} + \frac{1}{u_f} \cdot a \cdot r \tag{14}$$

$$\alpha_{\max} = -\frac{1}{u_f} \cdot (v - b \cdot r_{\max_2}) \;\Rightarrow\; r_{\max 2} = \frac{\alpha_{\max} \cdot u_f}{b} \tag{15}$$

The minimum of yaw rate limits $r_{\max 0}$, $r_{\max 1}$ and $r_{\max 2}$, (see Eq. (8), (10) and (15)) is denoted as $r_{\max} = \min(r_{\max 1}, r_{\max 2}, r_{\max 3})$. By implementing a constraint on the maximum yaw rate and maximum tire slip angle we indirectly impose a constraint on maximum vehicle slip angle.

Steering system model and rate constraints

For collision avoidance purposes the vehicle needs to be equipped with an active steering system. In this study, we consider a steer by-wire system (Figure 3). Following Werum, 2013, it is described by a second order transfer function

$$\frac{\delta}{I} = \frac{k}{J \cdot s^2 + D \cdot s + K} \tag{16}$$

where δ is wheel's steer angle, I the commanded motor current and *k=56.1, J=0.005146, D=0.07264, K=3.389* the steering system parameters. In Figure 4, the open

loop transient response of steering angle and steering rate for a unit step input is shown. As observed, the settling time is approximately 0.35 *s* considerable enough for maneuvers with short duration. In order to include the effect of steering rate in the equations of motion we assume that lateral velocity *v* is negligible, substitute Equations (12) and (13) in Equation (3) and differentiate once:

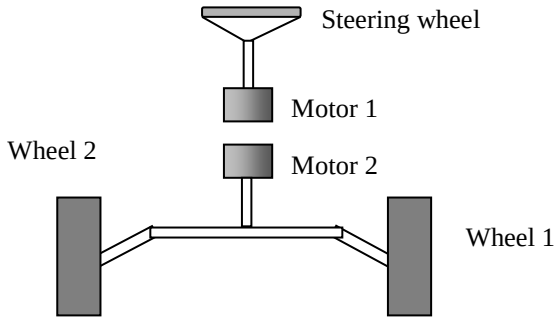

Figure 3. Steer by wire system

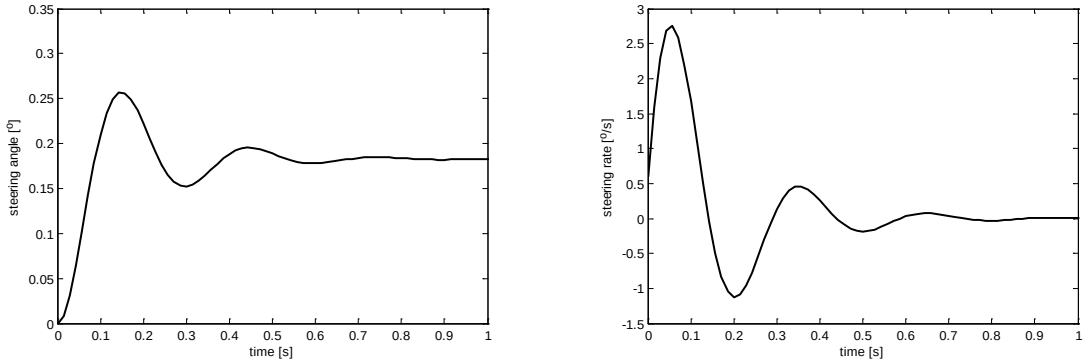

Figure 4. Steer angle (left) and steering rate (right) open loop transient response for a step input

$$\frac{d^2r}{dt^2}+\frac{a^2\cdot\overline{C}_{y1}+b^2\cdot\overline{C}_{y2}}{I_z\cdot u_f}\cdot\frac{dr}{dt}=\frac{a\cdot\overline{C}_{y1}}{I_z}\cdot\frac{d\delta}{dt} \qquad (17)$$

where $\overline{C}_y=\frac{F_{y0}(a)}{a}$ is the average tire stiffness. The transient response of angular jerk $\dddot{r}$ for a unit step input at two different vehicle speeds is shown in Figure (5). The maximum

angular jerk $\ddot{r}_{\max}\left(\dot{\delta}_{\max}, u_f\right)$ is mainly dependent on maximum steering rate $\dot{\delta}_{\max}$ and vehicle speed.

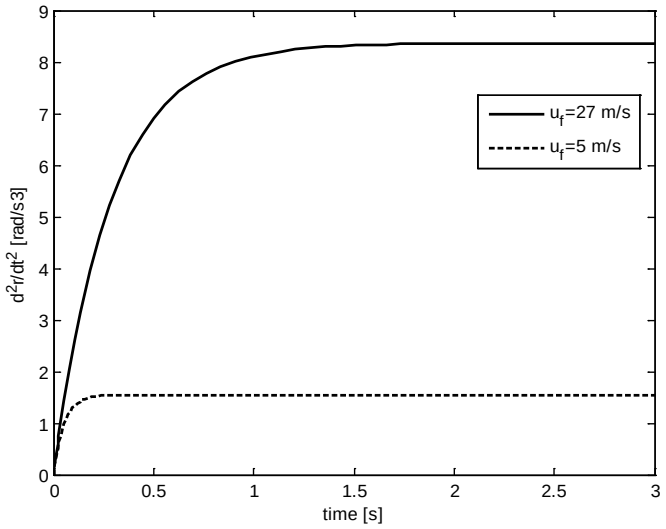

Figure 5. Transient response of vehicle's yaw acceleration rate for a steering rate step input for two different velocities

The inherent limitations of the TTVM model apply to the proposed method. It will not approximate vehicle motion well at very low speeds, during tight maneuvers or during high speed maneuvering where the influence of suspension geometry is critical. It is also known from Mitschke (2004) that the linear bicycle model is valid only when $F_{y\max} < \frac{1}{3} \cdot \mu \cdot F_z$, effectively for lateral accelerations up to 0.4 g's for dry road conditions and 0.05 g's on icy conditions.

Another limitation is the constant forward velocity u_f assumption. Tire forces in the direction of the velocity are neglected. As with yaw, tire forces (unless balanced) are expected to reduce velocity when slip angles are present. This is due to the fact that slip angles generate tire force components that oppose velocity. For small slip angles the influence is negligible but for high slip angles the effect is considerable. However, due to the fact that front and rear tyres' slip angles are bounded it is expected that their influence will be -in most cases- limited. In any case, other parameters such as aerodynamic resistance and engine-gearbox friction losses will also cause a reduction in forward velocity u_f. A reduction in forward velocity u_f means that the vehicle will cover less

distance both in longitudinal *X* and lateral direction *Y*. Thus, without consideration of a reasonable safety factor the vehicle might collide with another object.

Additionally, it is emphasized that the proposed method is also implementable for other lateral motion control systems e.g. differential braking system. In this case maximum jerk $\dddot{r}_{\max}$ will be defined by the dynamics of the differential braking system.

3. Finite element method

Planning EPs is a computationally demanding problem because a system of differential equations needs to be solved iteratively in real time. Since no reference trajectory, e.g. road lane, is available both states and inputs of the system are unknown during the maneuvering period. In order to reduce the computational load a finite element concept is proposed which recasts the problem into a deterministic linear algebraic one and thus eases calculations.

A schematic of the approach is shown in Figure 6. The total path is decomposed in *N* finite elements/segments. Each finite element is denoted with a number *n=1*…*N*, and has two nodes: the start node $\mathbf{n}_a$ and end node $\mathbf{n}_b$. The EP is constructed by joining end node $\mathbf{n}_b$ and start node $(\mathbf{n+1})_a$ of two consecutive finite elements **n** and **n+1**, for *n=1*:..:*N-1*.

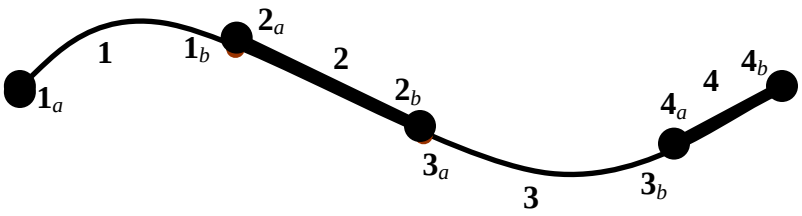

Figure 6. Emergency path decomposed into 4 finite elements

Each finite element is parameterized using two variables: time span $t_{n\,span}$ and the highest order constrained state variable. Time span $t_{n\,span}$ may be uniformly chosen by decomposing the total maneuvering time in *n* segments or by considering other parameters such as change of tire-road friction coefficient μ and road curvature. In this paper, angular jerk is the highest order constrained state variable and assumed constant in

each segment, $\ddot{r}_n = \alpha_{3n}$ for $t_n \in [0, t_{nspan}]$. In this context, angular acceleration $\dot{r}_n$, velocity r_n and position θ_n are:

$$\ddot{r}_n = \alpha_{3n} \tag{18}$$

$$\dot{r}_n = \int_0^{t_{nspan}} \ddot{r}_n \cdot dt = \alpha_{3n} \cdot t_n + \alpha_{2n} \tag{19}$$

$$r_n = \int_0^{t_{nspan}} \dot{r}_n \cdot dt = \frac{1}{2} \cdot \alpha_{3n} \cdot t_n{}^2 + \alpha_{2n} \cdot t_n + \alpha_{1n} \tag{20}$$

$$\theta_n = \int_0^{t_{nspan}} r_n \cdot dt = \frac{1}{6} \cdot \alpha_{3n} \cdot t_n{}^3 + \frac{1}{2} \cdot \alpha_{2n} \cdot t_n{}^2 + \alpha_{1n} \cdot t_n + \alpha_{0n} \tag{21}$$

where $t_n \in [0, t_{nspan}]$.

The states $y_n = \begin{bmatrix} \dot{r}_{n,a} & r_{n,a} & \theta_{n,a} & \dot{r}_{n,b} & r_{n,b} & \theta_{n,b} \end{bmatrix}^T$ at the boundaries of the finite element are expressed in matrix form as:

$$\mathbf{y_n} = \mathbf{A_n} \cdot \mathbf{x_n}$$

$$\mathbf{y_n} = \begin{bmatrix} \dot{r}_{n,a} & r_{n,a} & \theta_{n,a} & \dot{r}_{n,b} & r_{n,b} & \theta_{n,b} \end{bmatrix}^T$$

$$\mathbf{x_n} = \begin{bmatrix} a_{3n} & a_{2n} & a_{1n} & a_{0n} \end{bmatrix}^T \tag{22}$$

$$\mathbf{A}_n = \begin{bmatrix} 0 & 1 & 0 & 0 \\ 0 & 0 & 1 & 0 \\ 0 & 0 & 0 & 1 \\ t_{nspan} & 1 & 0 & 0 \\ 0.5 \cdot t_{nspan}^2 & t_{nspan} & 1 & 0 \\ 0.1667 \cdot t_{nspan}^3 & 0.5 \cdot t_{nspan}^2 & t_{nspan} & 1 \end{bmatrix}$$

The finite element matrix $\mathbf{A}_n$ constitutes the basis for joining subsequent elements and deriving the system's solution.

4. Solution method

A three step method is proposed for determining EPs. At each step the time grid is adapted – if necessary- in order to meet a design objective:

- **Step 1**: The EP problem is solved for a given maneuvering period. A uniform time grid is selected to standardize calculations and derive a fast solution. The discretization depends on the problem.
- **Step 2**: A check is being made whether the control input amplitude is the dominant constraint of the problem. If yes then the time grid points are relocated in order to minimize the control input amplitude. If not the time grid points are relocated in order to optimize the dynamic properties of the trajectory.
- **Step 3**: A check is being made whether maneuvering period can be significantly reduced. If positive then a one unknown optimization problem is solved using a fixed number of function evaluations.

It is important to notice that a solution to the problem already exists from the first step. The following steps seek to optimize the EP with respect to different objectives. A detailed description of the three steps follows.

Step 1: Solution with uniform finite elements

The path is decomposed in *N* uniform finite elements with the same time span $t_{n\,span}$. The EP is computed by solving the following linear system of equations:

$$\begin{aligned}
&\mathbf{y}_{bc} = \mathbf{A}\cdot\mathbf{x}_u \\
&\mathbf{y}_{bc} = \left[\dot{r}_{1,ades} \quad r_{1,ades} \quad \theta_{1,ades} \quad \ldots \quad \dot{r}_{n,ndes} \quad r_{n,bdes} \quad \theta_{n,bdes}\right] \\
&\mathbf{x}_u = \left[a_{31} \quad a_{21} \quad a_{11} \quad a_{01} \quad \ldots \quad a_{3n} \quad a_{2n} \quad a_{1n} \quad a_{0n}\right] \\
&\sum_{i=1}^{N} t_{nspan} = T
\end{aligned} \tag{23}$$

where $\mathbf{y}_{bc}$ is the vector of boundary conditions, $\mathbf{x}_u$ is the vector of unknown coefficients and **A** the system's matrix. It is obvious that with different path

decomposition Equation (23) would give another solution. There are infinite EPs that satisfy the boundary conditions and which can be computed using the FE method. The reason for using, in the first step, uniform path decomposition is because then a) all elements share the same matrix $\mathbf{A}_n$ and b) the linear system of equations (23) can be solved with less computational burden.

Vectors $\mathbf{x}_u$ and $\mathbf{y}_{bc}$ as well as system matrix $\mathbf{A}$ are formed by joining subsequent elements. In particular, we use the desired conditions at beginning ($t=0$) and end ($t=T$) of the EP:

$$\dot{r}(t=0)=\dot{r}_{1,ades},\ r(t=0)=r_{1,ades},\theta(t=0)=\theta_{1,ades} \qquad (24)$$
$$\dot{r}(t=T)=\dot{r}_{N,bdes},\ r(t=T)=r_{N,bdes},\ \theta(t=T)=\theta_{N,bdes}$$

as well as the desired state values s_i for a number of additional (problem dependent) points i ($t=t_i,\ t_i \in [0,T]$)

$$s(t=t_i)=s_{i,des} \qquad (25)$$

where $s_{i,des}$ can be the angular acceleration $\dot{r}_i$, angular velocity r_i, angular position θ_i or lateral displacement Y_i. For assembling the system matrix $\mathbf{A}$ we use the continuity equations between subsequent elements

$$\dot{r}_{n,b}=\dot{r}_{n+1,a},\ r_{n,b}=r_{n+1,a},\ \theta_{n,b}=\theta_{n+1,a} \qquad (26)$$

and the desired lateral displacement Y_{des} at the end ($t=T$) of the EP:

$$\sum \delta Y_n = Y_{des} \qquad (27)$$

where δY_n is the lateral displacement of a finite element:

$$\delta Y_n = \int_0^{t_n s_{pan}} u_f \cdot \sin(\theta_n) \cdot dt \approx u_f \cdot \int_0^{t_n s_{pan}} \theta_n \cdot dt \tag{28}$$
$$= \left(\frac{1}{24} \cdot \alpha_{3n} \cdot t_n^4 + \frac{1}{6} \cdot \alpha_{2n} \cdot t_n^3 + \frac{1}{2} \cdot \alpha_{1n} \cdot t_n^2 + \alpha_{0n} \cdot t_n \right) \cdot u_f$$

In Equation (28) the incremental lateral displacement δY_n is linearized by assuming $\sin(\theta_n) \approx \theta_n$. The proposition is valid only for small angles $\theta_n \leq 5^o$. For larger angular displacement θ_n the path has to be decomposed into a greater number of finite elements.

The total number of unknowns is N_u=4·N while the number of constraints N_c= $3 \cdot (N+1) + K + 1$, where $K \leq N-3$ is the number of state conditions defined at intermediate points *i*. By equating $N_u = N_c$ the number N of finite elements for which a determinist problem results is found.

Step 2: Time grid points relocation

In the second step the time grid points are relocated in order to improve the EP either with respect to the maximum control input amplitude or with respect to its dynamic properties. First, it is examined whether control amplitude is the dominant constraint:

$$\max_{n=1,\ldots,N}(|a_{3n}|) \begin{cases} > \ddot{r}_{\max} \rightarrow \textit{relocation}, & \min(\max \alpha_{0,n}) \\ < \ddot{r}_{\max} \rightarrow \textit{relocation}, & \min(\max \dot{r}_n) \end{cases} \tag{29}$$

If the control amplitude exceeds the predefined threshold $\ddot{r}_{\max}(\dot{\delta}_{\max}, u_f)$ then the time grid is adapted in such a way that the differences between input amplitudes are minimized. The concept is shown in Figure 7. The formula used is based on (Kanarachos, [2009]) and given by:

$$t'_{nspan} = 0.85 \cdot \frac{|a_{3n}|}{\sum |a_{3n}|} \cdot T + 0.15 \cdot t_{nspan} \tag{30}$$

where t'_{nspan} is the new time span for finite element *n*.

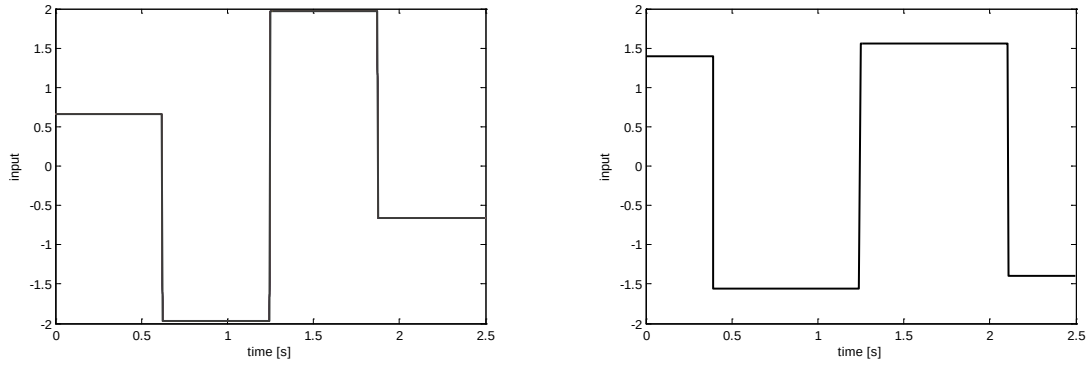

Figure 7. Resulting inputs for uniform coarse grid (left) and adapted one (right)

If the control amplitude doesn't exceed the predefined threshold $\ddot{r}_{\max}\left(\dot{\delta}_{\max}, u_f\right)$ then the time grid points are relocated in such a way that the maximum angular velocity $\left|r_{n,\max}\right|$ is minimized. The following empirical formula is used for computing the new finite element time span t'_{nspan}:

$$t'_{nspan} = 0.9 \cdot \frac{\left(r_{n,b} - r_{n,a}\right)^2}{\sum \left(r_{n,b} - r_{n,a}\right)^2} \cdot T + 0.1 \cdot t_{nspan} \tag{31}$$

Step 3: Minimum maneuvering period

In steps 1 & 2 the EP is computed for a chosen manoeuvring period *T* which is usually determined by the time to collision (TTC) algorithm. In case the maximum control input amplitude $\max\left(\left|a_{3n}\right|\right)$ or the maximum angular velocity $\left|r_{n,\max}\right|$ exceed the allowable limits then the maneuver isn't feasible and a collision mitigation action should take place. In the opposite case, a time window –valuable for other purposes such as situational awareness

and decision making- exists before the collision avoidance maneuver is initiated. In order to calculate the minimum manoeuvring time $T_{\min}$, for which one or more of the states or inputs are at the limit ($\max(|\ddot{r}_n|)_{T\min} = \ddot{r}_{\max}$ or $\max(|r_n|)_{T\min} = r_{\max}$) an optimization problem has to be solved. The trick proposed in this study is to seek the optimized solution in step three (3) by keeping the solution pattern $\frac{t_n}{\sum t_n}$ computed in step two (2). By following this approach the problem becomes scalable and has only unknown $T_{\min} = \sum t_n$:

$$f(T) = \min\left(\max\left(|\ddot{r}_n|_T - \ddot{r}_{\max}\right), \max\left(|r_n|_T - r_{\max}\right)\right) \quad (32)$$

$$T_{\min} = \min_T f(T), T \in [1, 4.5]$$

In this study, the optimization problem is solved using Matlab routine *fminunc*, a combination of BFGS quasi-Newton method with a polynomial line search procedure. Other Matlab routines such as *fmincon* (interior point) and *fminsearch* (simplex search) have been also tested but *fminunc* had the best performance. The optimized solution is found with reasonable accuracy in maximum 5 iterations (10 function evaluations) independent of the starting solution. A further computational advantage of the proposed method is that maximum values of yaw acceleration $\dot{r}_{n,\max}$ and yaw velocity $r_{n,\max}$ are easily checked since they are described by a first and second order polynomial respectively.

A schematic of the proposed algorithm is shown in the following figure:

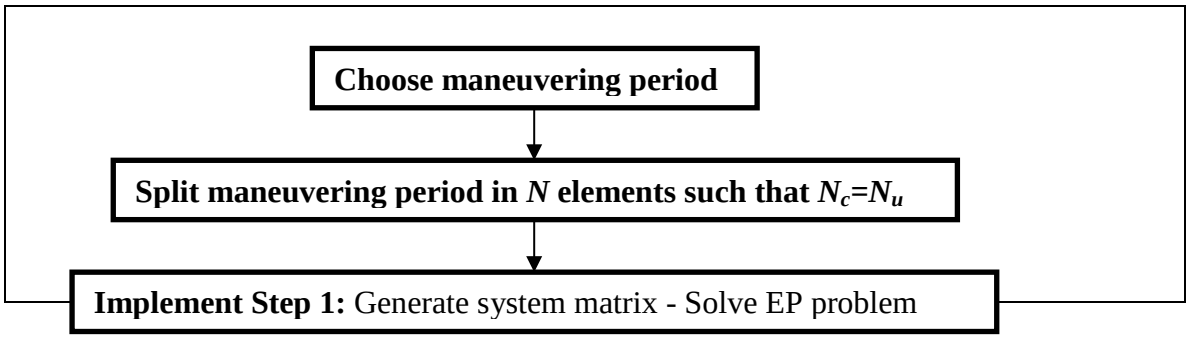

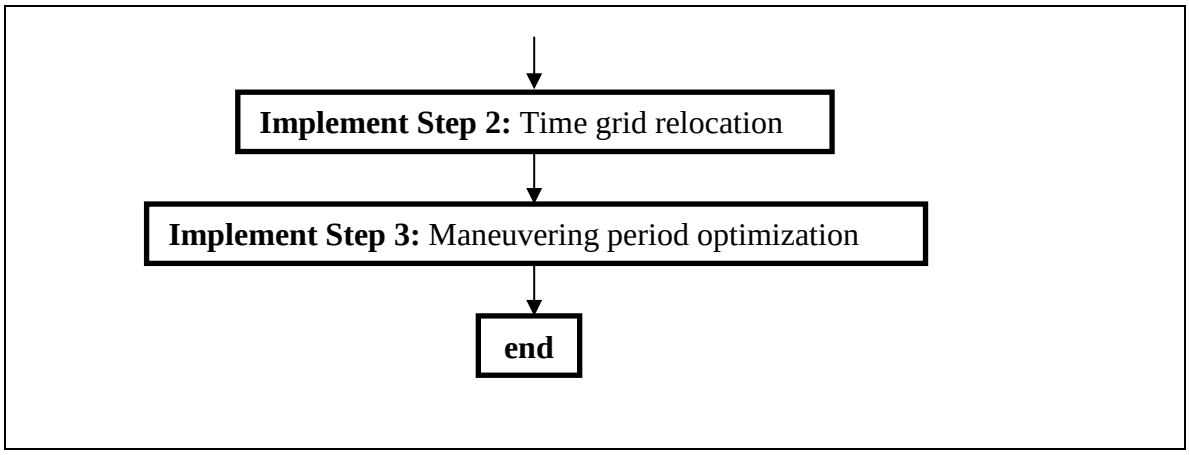

Figure 8. Schematic of proposed algorithm

5. Numerical examples – Driving scenarios

The proposed method's performance has been examined for an extensive number of driving scenarios in Matlab/Carsim simulation environments. The numerical examples are based on the vehicle data listed in Table 1 and tire parameters listed in Table 2. In the following three driving scenarios which highlight the features of the proposed method are presented and discussed.

Driving scenario 1: Emergency maneuver with zero boundary conditions: $Y_{des} = 3\,m$ and $T = 2.12\ s$

In the first driving scenario the vehicle moves longitudinally with a speed $u_f = 30\ m/s$ on a wet road surface ($\mu = 0.5$) when an obstacle at distance $d = 63.6\,m$ suddenly appears in its direction of travel. To avoid the collision the vehicle has to displace laterally by $Y_{des} = 3\,m$. A per wheel lateral load transfer limit $(\delta F_{zi})_{\max} = 2000\,N$ has been set to ensure no wheel lift off and stability.

In Figure (9) the results obtained for two different EP planning methods are shown. On the left part the results using the polynomial-sigmoid (P-S) method Keller et al. (2011) are illustrated and on the right the ones using the proposed method (FE). Figure (9) is composed of multiple parts which show in part (a) the lateral displacement Y, in part (b) the lateral velocity dY/dt and in part (c) the lateral acceleration dY^2/dt^2 of the

vehicle for the same maneuvering period $T = 2.12$ *s*. With the P-S method the maximum lateral acceleration $\ddot{y}_{\max}$ is 5 m/s^2 while with the proposed one 4.42 m/s^2. Thus, with the proposed method the maneuver can be accomplished in less time. The solution $T^* = 1.99$ *s* is found –with reasonable accuracy - after maximum ten function evaluations independent of the starting point $T \in [1,4.5]$ *s* .

a)

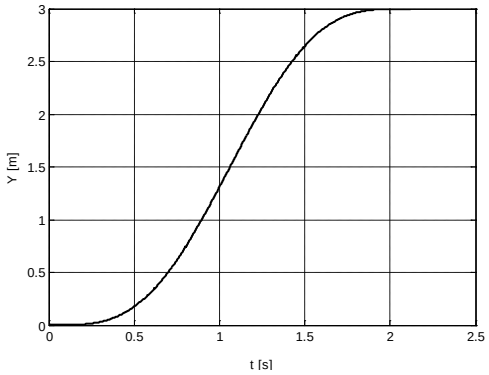

b)

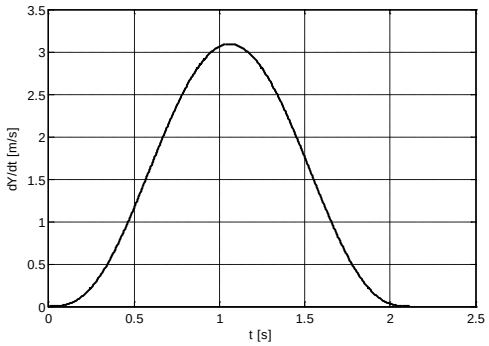

c)

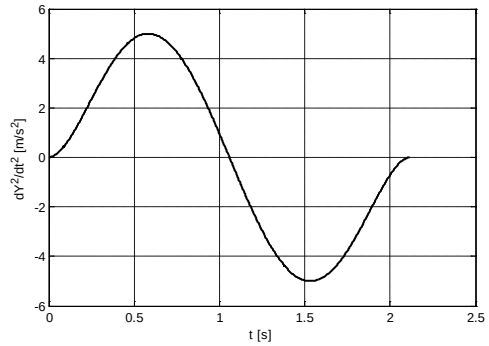

a)

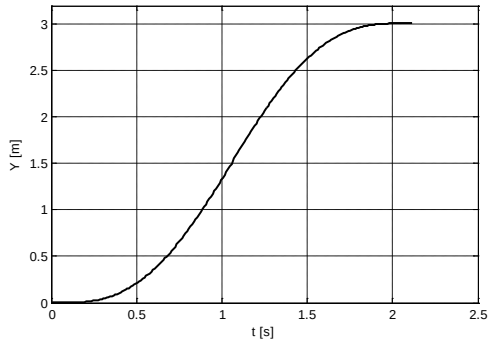

b)

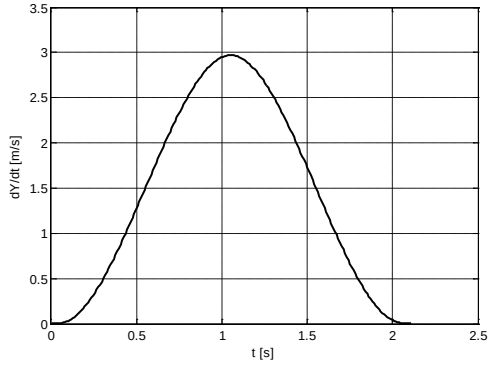

c)

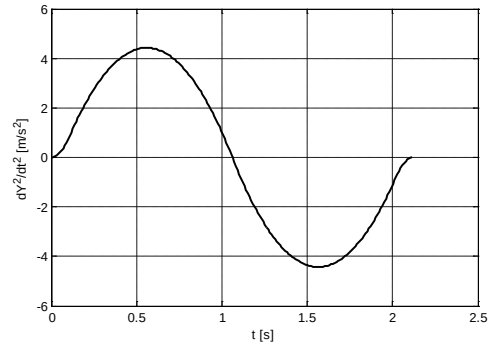

Figure 9. Optimized EP solution for the second driving scenario using P-S (left) and proposed (right) methods a) lateral displacement b) lateral acceleration and c) lateral jerk versus time

The convergence plot for the optimization algorithm for two different starting points T_{start}=2.12 s and T_{start}=2.9 *s* are shown in Figure 10. The optimized maneuvering time found *s* in both cases is $T^* = 1.99$ after three iterations.

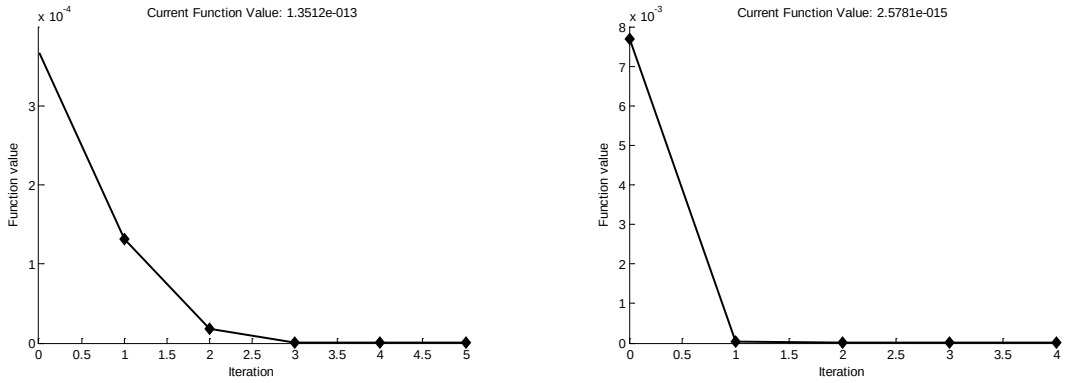

Figure 10. Convergence plot for starting point T_{start}=2.12 s (left) and T_{start}==2.7 s (right)

Driving scenario 2: Emergency maneuver with non zero boundary conditions: $Y_{des} = 4\,m$, $\theta(t=0) = 0.15\,rad$, $\theta_{des} = 0.017\,rad$ and $T = 2.5\,\mathrm{s}$

In the second driving scenario the vehicle moves with a speed $u_f = 20\,m/s$ on a wet road surface ($\mu = 0.5$) when an obstacle at distance $d = 40\,m$ suddenly appears in the direction of travel. To avoid the collision the vehicle has to displace laterally by $Y_{des} = 4\,m$. At *t*=0 the angle is $\theta_{1,a}(t=0) = 0.15\,rad$ and at maneuver's end the desired angle is $\theta_{des} = 0.017\,rad$. A per wheel lateral load transfer limit $(\delta F_{zi})_{\max} = 2000\,N$ has been set to ensure no wheel lift off and stability.

In Figure (11) the results obtained for two different EP planning methods are shown. On the left part the results using the polynomial-sigmoid (P-S) are illustrated and on the right the ones using the proposed method. Figure (11) is a multi-part figure which shows a) lateral displacement Y, b) lateral acceleration dY^2/dt^2 and c) lateral jerk d^3Y/dt^3 of the vehicle during the maneuvering period. The computed minimum maneuvering time

T^* with the P-S method is $2.5s$ *s*, while with the proposed method 2.1 *s*. With the proposed method the solution is found –with reasonable accuracy - after maximum three iterations, independently of the starting point $T \in [1,4.5]\, s$.

a)

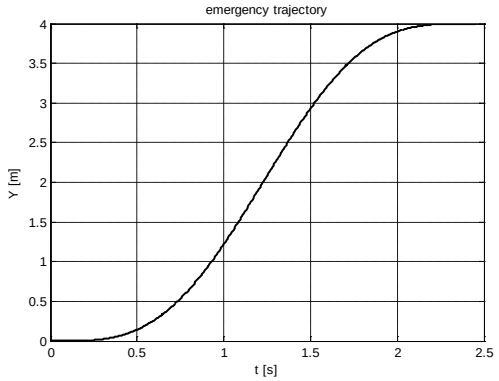

a)

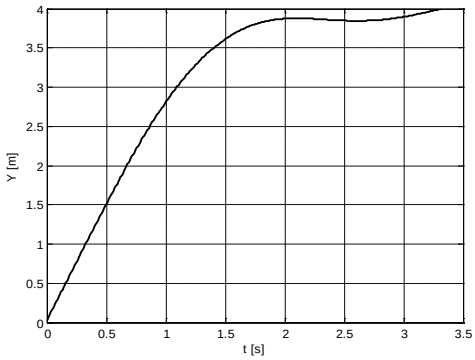

b)

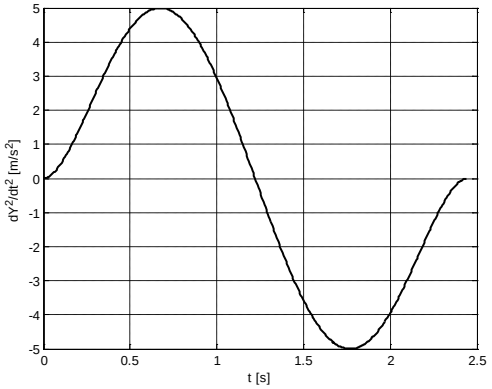

b)

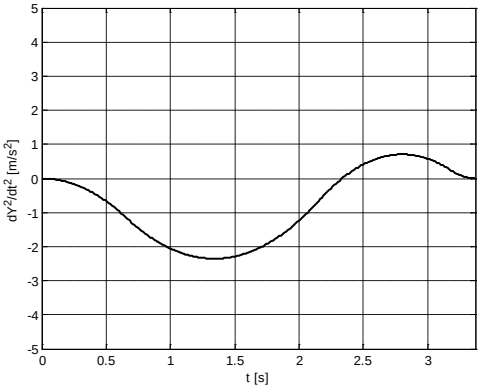

c)

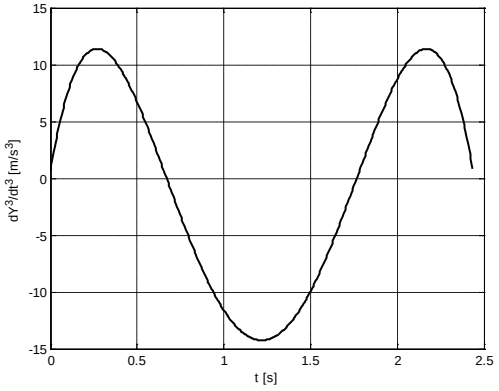

c)

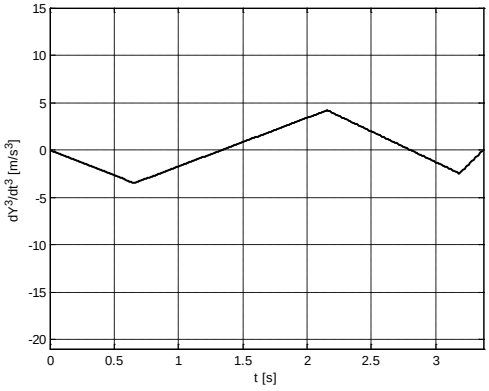

Figure 11. Optimized EP solution for the second driving scenario using P-S (left) and proposed (right) methods a) lateral displacement b) lateral acceleration and c) lateral jerk versus time

As observed with the P-S method maximum lateral acceleration $\left(dY^2/dt^2\right)_{\max}$ is 5 m/s^2 and maximum lateral jerk $\left(dY^3/dt^3\right)_{\max}$ 15 m/s^3. Contrary, using the FE method the maximum lateral acceleration is 2.35 m/s^2 and maximum lateral jerk 4.2 m/s^3. Both values are considerably lower compared to the P-S method.

In order to assess the influence of the improved EP on vehicle performance a further analysis has been conducted in Carsim. In particular, a vehicle model with fully described suspension properties and a proportional-derivative P-D with preview path tracking controller was instructed to follow the EP planned by both methods. The initial vehicle state is derived by driving the vehicle on a predefined trajectory before the emergency maneuver starts. In Figures 12a and 12b the planned Y_{plan} and realized Y_{real} vehicle trajectories are shown. The planned trajectory for $0 \le t \le 3.5\,s$ is the same for both vehicles and is used to derive non zero vehicle states when the emergency maneuver starts at $t = 3.5\,s$. As expected the vehicle response is different for the two different planned emergency paths. At $t = 6\ s,$ the errors for case 1 are $\left(Y_{plan} - Y_{real}\right)_1 = 2.7\,m$ and $\left(\theta_{plan} - \theta_{real}\right)_1 = 12.4^o$, while for case 2 $\left(Y_{plan} - Y_{real}\right)_2 = 0.02\,m$ and $\left(\theta_{plan} - \theta_{real}\right)_2 = 0.5^o$ respectively. The discrepancies between planned and realized trajectories are due to the unmodelled vehicle dynamics which has been neglected in the planning phase. It is highlighted that although both vehicles reach the limits of lateral acceleration $a_{y\max} = 4.5\,m/s^2$, the duration at the limits is different. With the F-E method the duration is minimal and much shorter than with the P-S method. Furthermore, the load transfer δF_{zi} in both cases is different. In the first case the maximum load transfer is $\left(\delta F_{zi}\right)_{\max,2} = 2030\,N$, while in the second case $\left(\delta F_{zi}\right)_{\max,2} = 1820\,N$. Table 3 summarizes the numerical results.

a) a)

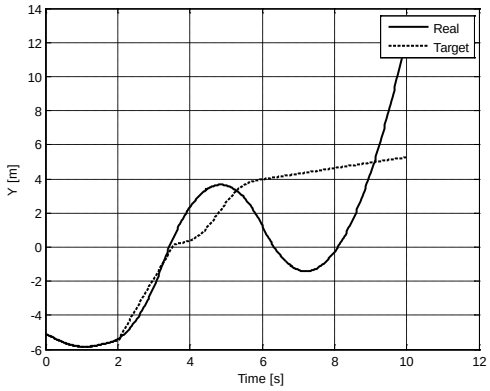
Real
Target
Y [m]
Time [s]

b)

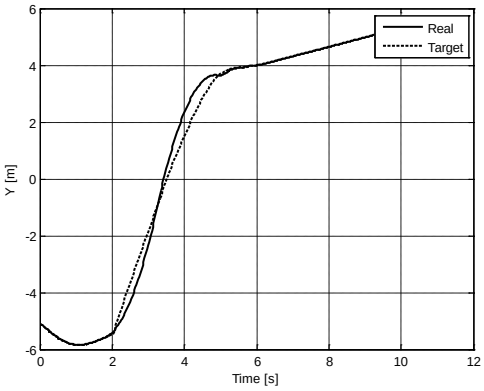
Real
Target
Y [m]
Time [s]

b)

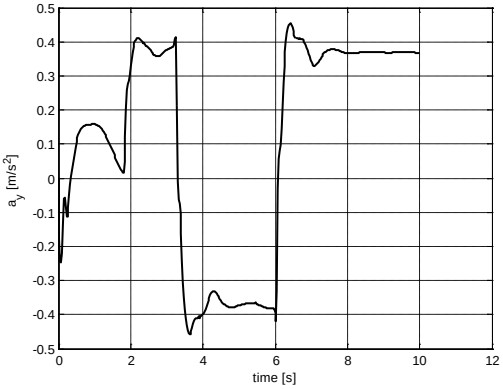
a_y [m/s^2]
time [s]

c)

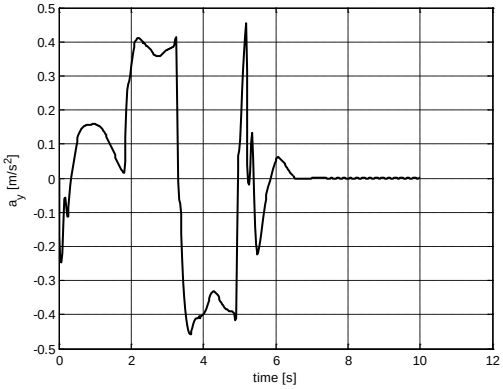
a_y [m/s^2]
time [s]

c)

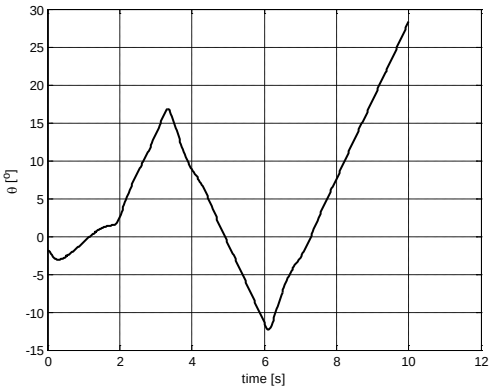
θ [°]
time [s]

d)

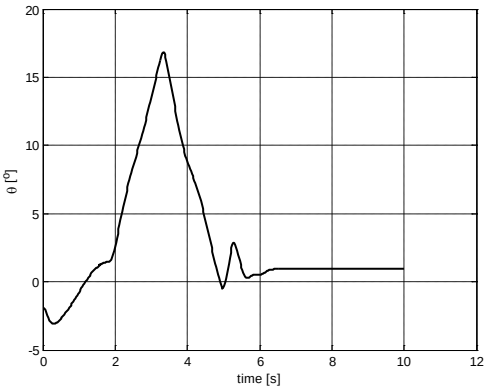
θ [°]
time [s]

d)

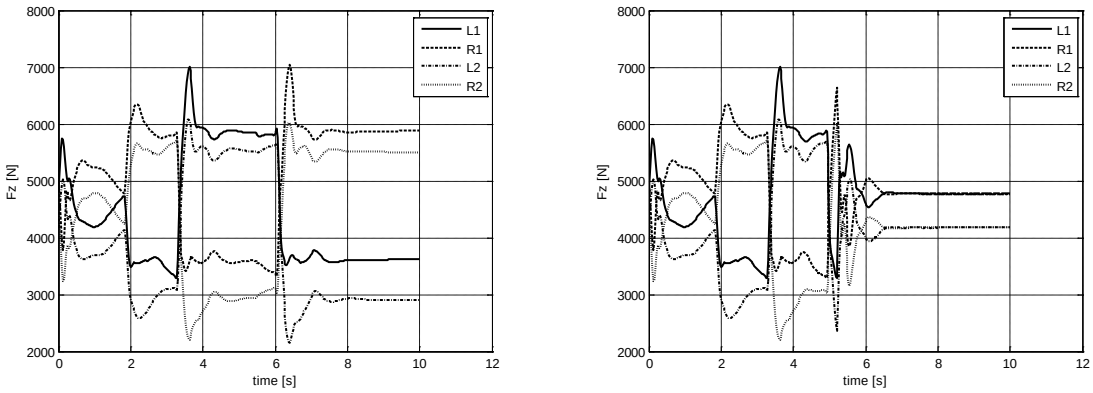

Figure 12. Vehicle response using P-S (left) and proposed (right) method for the second driving scenario: a) $t-Y$ graph, b) $t-a_y$ graph, c) $t-\theta$ graph, d) $t-F_z$ graph

Table 3 Results for second driving scenario

Name	**P-S method**	**FE method**
Maximum lateral acceleration $\left(dY^2/dt^2\right)_{\max}$ $[m/s^2]$	5	2.35
Maximum lateral jerk $\left(dY^3/dt^3\right)_{\max}$ $[m/s^3]$	15	4.2
$\left(Y_{plan}-Y_{real}\right)_{t=6s}$ $[m]$	2.7	0.02
$\left(\theta_{plan}-\theta_{real}\right)_{t=6s}$ $[^o]$	12.4	0.5
$\left(\delta F_{zi}\right)_{\max}$ $[N]$	2030	1820
End boundary conditions fulfillment	No	Yes

Driving scenario 3: Emergency maneuver with non zero boundary conditions: $Y_{des}=3\,m$, $\dot{\theta}_{N,bdes}=0.16\,rad/s$ *and* $\theta_{N,bdes}=3^o$

In the third driving scenario the vehicle moves longitudinally with a speed $u_f=30\,m/s$ on a wet road surface ($\mu=0.5$) when an obstacle at distance $d=70\,m$ suddenly appears in its direction of travel. To avoid the collision the vehicle has to displace laterally by $Y_{des}=3\,m$. At the end of the maneuver the road which the vehicle has to follow is not straight but curved (Figure 14). The desired end state conditions are therefore

$\dot{\theta}_{N,bdes} = 0.16\, rad/s$ *and* $\theta_{N,bdes} = 3^o$. A per wheel lateral load transfer limit $(\delta F_{zi})_{\max} = 2000\, N$ has been set to ensure no wheel lift off and stability.

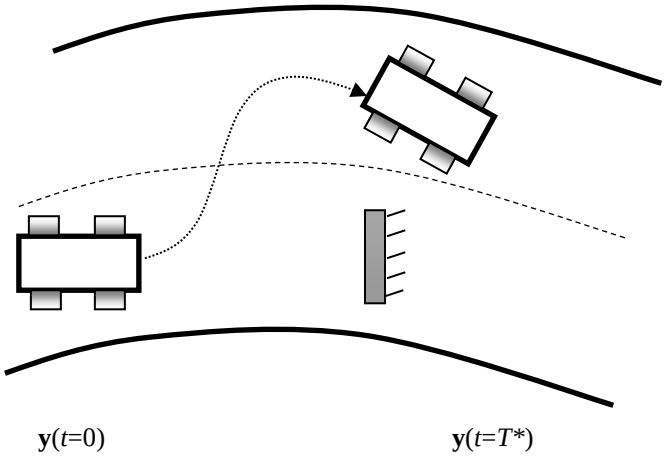

Figure 13. Obstacle avoidance manoeuvre with curvature constraints

In Figure (14) the EP results using the P-S (left) and FE (right) methods are shown. In a) lateral displacement Y, b) lateral acceleration dY^2/dt^2 and c) lateral jerk of the vehicle d^3Y/dt^3 are shown. In P-S the desired end boundary conditions aren't met. Maximum lateral acceleration $(dY^2/dt^2)_{\max}$ is 4.5 m/s^2 and maximum lateral jerk $(dY^3/dt^3)_{\max}$ is 16.5 m/s^3. In the FE method $(dY^2/dt^2)_{\max}$ =5 m/s^2 and $(dY^3/dt^3)_{\max}$ =10 m/s^3.

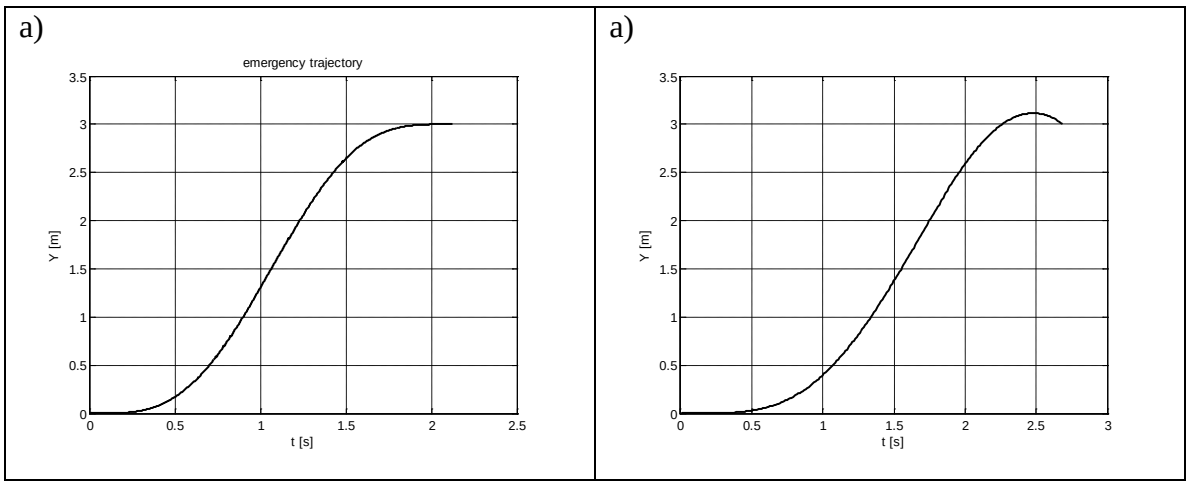

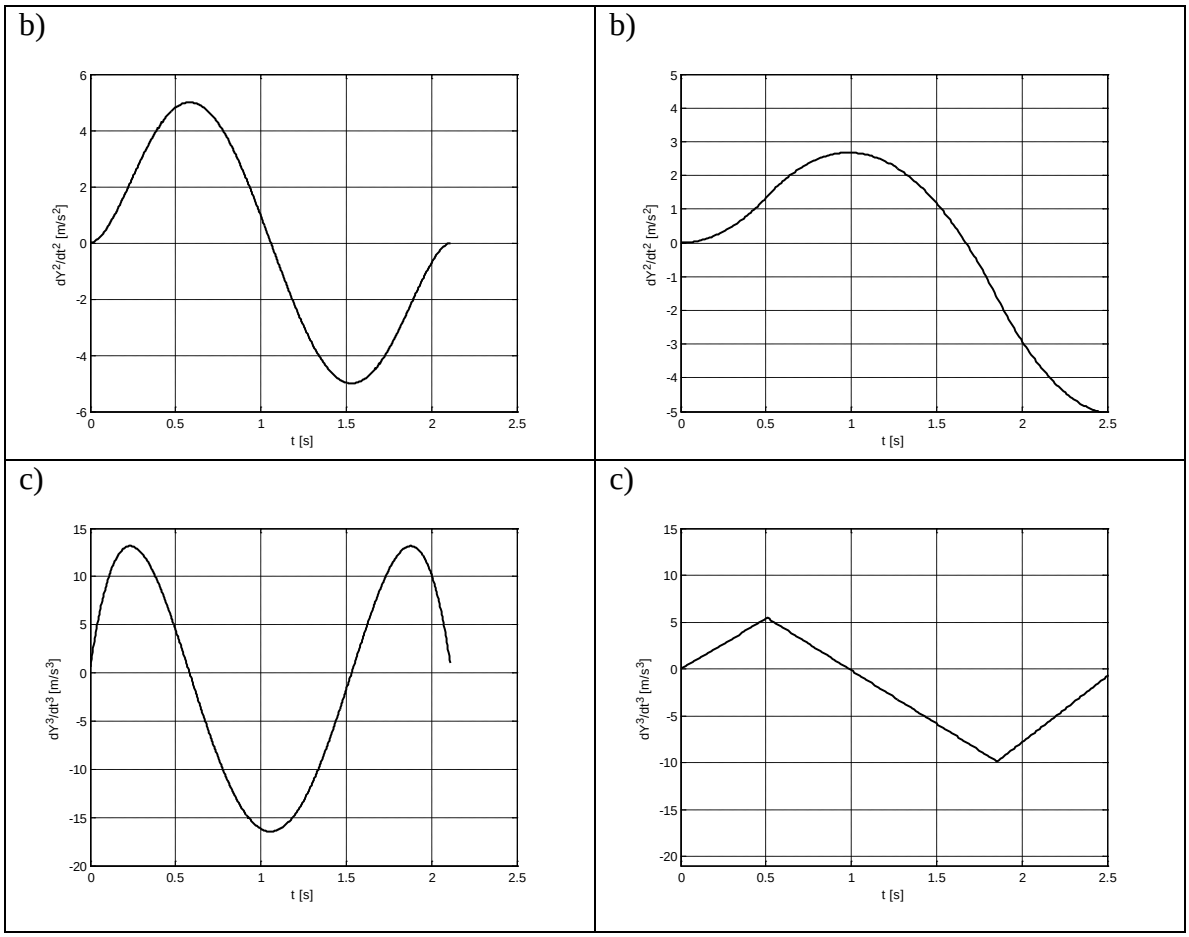

Figure 14. Optimized EP solution for the third driving scenario using P-S (left) and proposed (right) method: a) lateral displacement b) lateral acceleration and c) lateral jerk versus time

Table 4 Results for third driving scenario

Name	**P-S method**	**FE method**
Maximum lateral acceleration $\left(dY^2/dt^2\right)_{\max}$ [m/s^2]	4.5	5
Maximum lateral jerk $\left(dY^3/dt^3\right)_{\max}$ [m/s^3]	16.5	10
End boundary conditions fulfillment	No	Yes

6. Sensitivity analysis

In previous section it was shown that the FE method performs satisfactorily for a number of complex driving scenarios with arbitrary boundary conditions and is -thus to some extent- robust. In this section, a sensitivity analysis will show that the method performs also robustly with respect to uncertain parameters such as friction coefficient μ .

Tire-road friction coefficient μ is rarely precisely known and usually estimated by performing a rough classification of the road condition as icy, snowy, wet or dry. Thus, it is of high relevance to know how the method performs if the friction coefficient is over or under-estimated. In this context, we conducted a parametric analysis for a straight line emergency maneuver in which the friction coefficients μ is uncertain and varies $0.4 \le \mu < 0.6$. The forward speed of the vehicle is $u_f = 25 m/s$ when the emergency maneuver starts.

In the left part of Figure 15 the planned EPs are shown, while in Table 5 the differences between the numerical results at four time instants $t = 0.5,1,1.5,2\ s$ are highlighted. As observed at $t = 0.5\ s$ and $t = 2\ s$ the results are almost identical while at $t = 1\ s$ and $t = 1.5\ s$ the difference in lateral displacement is on average 0.3 *m*. On the right part of Figure 15 the FE solution for the three different friction coefficients is shown. On x–axis is variable $\xi = \frac{t}{T}$ and y-axis the angular acceleration $\ddot{r}$ represented. As observed all solutions share the same pattern; only the amplitude changes as a function of the friction coefficient μ. It is possible, therefore, to easily predict the probable coverage area of the vehicle under the assumption that a statistical estimate of the friction coefficient μ exists.

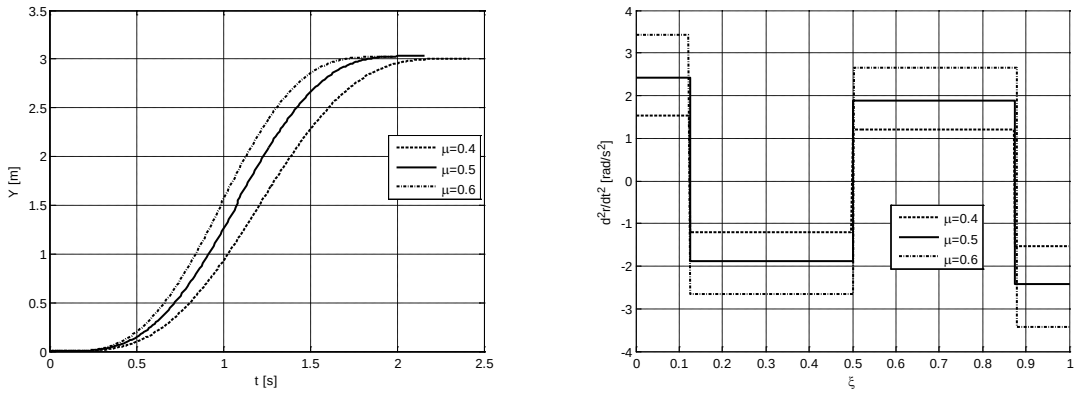

Figure 15. EP solution for three friction coefficients: $\mu = 0.4$ (dashed line), $\mu = 0.5$ (solid) and $\mu = 0.6$ (dash dotted line)

Table 5 Sensitivity analysis results

Name	$\mu = 0.4$	$\mu = 0.5$	$\mu = 0.6$
$Y_{t=0.5s}\ [m]$	0.10	0.15	0.20
$Y_{t=1s}\ [m]$	0.94	1.26	1.57
$Y_{t=1.5s}\ [m]$	2.28	2.66	2.85
$Y_{t=2s}\ [m]$	2.95	3.02	3.02

7. Conclusions – Future research directions

In this paper a methodological framework for computing emergency maneuvers in complex driving scenarios with arbitrary boundary conditions is presented. The main contribution is a method to a) decompose the emergency maneuver in standardized finite elements and b) efficiently formulate the dynamic optimization problem into a sequential algebraic one. In particular, a three step solution procedure is proposed.

In the first step, the problem is solved for a given maneuvering period with a uniform time grid. The number of finite elements needed for transforming the dynamic optimization problem into a deterministic algebraic one is defined and a solution is obtained. In the second step, the dynamic properties of the computed path are evaluated – including the feasibility - and a recalculation of the emergency maneuver is performed in order to optimize it with respect to the dominant constraint. This is achieved by adapting

the time grid accordingly. In the third step, the minimum maneuvering time is computed in a few iterations using a novel optimization strategy.

Our future research activities include the extension of the proposed methodological framework for combined braking and steering driving scenarios in which an automated decision has to be made with respect to the driving strategy.

References

1. Arora, S., Dhaliwal, S.S., Kukreja, V.K. (2006) 'Application of orthogonal collocation on finite elements for solving non-linear boundary value problems', *Applied Mathematics and Computation*, Vol. 180, No. 2, pp. 516-523.
2. Brandt, T., Sattel, T., Wallaschek, J. (2007) 'Towards vehicle trajectory planning for collision avoidance based on elastic bands', *International Journal of Vehicle Autonomous Systems*, Vol. 5, pp. 28-46.
3. Gray, A., Yiqi Gao, Lin, T., Hedrick, J.K., Tseng, H.E., Borrelli, F. (2012) 'Predictive control for agile semi-autonomous ground vehicles using motion primitives', *Proceedings of the American Control Conference 2012*, pp. 4239-4244, 27-29 June 2012
4. Isermann, R., Mannale, R., Schmitt, K. (2012) 'Collision-avoidance systems PRORETA: Situation analysis and intervention control', *Control Engineering Practice*, Vol. 20, No.11, pp. 1236-1246.
5. Kanarachos, S. (2009) 'A new method for computing optimal obstacle maneuvers of vehicles', *International Journal of Vehicle Autonomous Systems*, 2009, Vol. 7, No. 1, pp. 73-95.
6. Kanarachos, S. (2013) 'Design of an intelligent feed forward controller system for vehicle obstacle avoidance using neural networks', *International Journal of Vehicle Systems Modelling and Testing*, Vol. 8, No.1, pp. 55 – 87.
7. Keller, C.G., Thao Dang, Fritz, H., Joos, A., Rabe, C., Gavrila, D.M. (2011) 'Active Pedestrian Safety by Automatic Braking and Evasive Steering', *IEEE Transactions on Intelligent Transportation Systems*, Vol.12, No.4, pp.1292-1304, Dec. 2011
8. Mitschke, M. and Wallentowicz, H. (2004), 'Dynamik der Kraftfahrzeuge', Spinger, 2004
9. Pacejka, B. (2005) 'Tire and Vehicle Dynamics' *Society of Automotive Engineers*, Warrendale
10. R. Rajamani, Vehicle Dynamics and Control - Chapter 8: Electronic Stability Control, Springer, New York, 2012

11. Shim, T. and Ghike, C. (2007) ‘Understanding the limitations of different vehicle models for roll dynamics studies’, Vehicle System Dynamics: International Journal of Vehicle Mechanics and Mobility, 45:3, 191-216
12. Shim, T., Adireddy G. and Yuan, H. (2012) ‘Autonomous vehicle collision avoidance system using path planning and model-predictive-control-based active front steering and wheel torque contro’, *Proceedings of the Institution of Mechanical Engineers, Part D: Journal of Automobile Engineering*, Vol. 226, pp. 767-778.
13. Solsvik, J., Jakobsen, H. (2012) ‘Effects of Jacobi polynomials on the numerical solution of the pellet equation using the orthogonal collocation, Galerkin, tau and least squares methods’, *Computers & Chemical Engineering*, Vol. 39, pp. 1-21.
14. Snider, JM. (2009) ‘Automatic Steering Methods for Autonomous Automobile Path Tracking’, *CMU-RI-TR-09-08 report*, Carnegie Mellon University
15. Vaferi, B., Salimi, V., Dehghan Baniani, D., Jahanmiri, A., Khedri, S. (2012) ‘Prediction of transient pressure response in the petroleum reservoirs using orthogonal collocation’, *Journal of Petroleum Science and Engineering*, Vol. 98–99, pp. 156-163.
16. Werum, G., 2013 ‘Steering actuator sizing of prototype electric one-seater’, *Master’s Thesis*, Chalmers University of Technology
17. Yang, X., Zhang, H., Xu, D. (2014) ‘Orthogonal spline collocation method for the two-dimensional fractional sub-diffusion equation’, *Journal of Computational Physics*, Vol. 256, No. 1, pp. 824-837.